Supramolecular Self-Assembled Ni(II), Fe(II), and Co(II) ABA Triblock Copolymers

Manuela Chiper,[†] Michael A. R. Meier,[†] Daan Wouters,[†] Stephanie Hoeppener,[†] Charles-André Fustin,[‡] Jean-François Gohy,[‡] and Ulrich S. Schubert*[,†,§]

Laboratory of Macromolecular Chemistry and Nanoscience, Eindhoven University of Technology and Dutch Polymer Institute (DPI), P.O. Box 513, 5600 MB Eindhoven, The Netherlands; Unité CMAT and CERMIN, Université catholique de Louvain, Place L. Pasteur 1, 1348 Louvain-la-Neuve, Belgium; and Laboratory of Organic and Macromolecular Chemistry, Friedrich-Schiller-Universität Jena, Humboldtstr. 10, D-07743 Jena, Germany

Received August 21, 2007; Revised Manuscript Received January 7, 2008

ABSTRACT: The self-assembly of amphiphilic metallo-supramolecular A-*b*-B-*b*-A triblock copolymers containing a B block formed from a bisfunctional terpyridine monomer and an A block based on a monofunctional terpyridine polymer is described. These polymers have been prepared by a polycondensation approach, based on metal–ligand complexation, in which the molecular weight of the central B block has been controlled by the addition of a monofunctional chain-stopper A. Details for the preparation of the A-*b*-B-*b*-A triblock copolymers based on the $tpy_2Ni(II)$, $tpy_2Fe(II)$, and $tpy_2Co(II)$ connectivity are given. The influence of the different binding strength of Ni(II), Fe(II), and Co(II) metal ions with terpyridine ligands on the metallo-polycondensation reaction and on the micellization behavior of those materials was studied. Micelles of the obtained block copolymers were prepared and studied by DLS and cryo-TEM.

Introduction

Inspired by nature, supramolecular chemistry has become one of the most studied topics in chemistry in the past years. Nowadays, polymers containing supramolecular binding units are synthetically accessible. The combination of macromolecular and supramolecular chemistry opens ways to obtain new functional materials that can be designed for a specific application by applying state-of-the-art controlled and living polymerization techniques teamed up with organic synthesis for the introduction of functional moieties into the polymer architecture. These supramolecular polymers can generally be defined as polymer chains of small molecules held together via reversible, noncovalent bonds.[1,2] The most outstanding examples of supramolecular polymers can be found in hydrogen-bonded systems,[3–6] systems based on metal–ligand interactions,[7–9] and systems that exploit ionic interactions.[10–12] All of these noncovalent interactions have certain advantages and disadvantages. Concerning metal–ligand interactions, the adjustability of their binding strength in a rather broad range (approximately between 25% and 95% of a covalent C−C bond, with a bond energy of 350 kJ/mol)[13] as well as their directionality can be considered an advantage, whereas the toxicity of some transition metal ions is a definite disadvantage. Hydrogen-bonding motifs, on the other hand, can generally be considered as less toxic but span a considerably smaller range of binding strengths (approximately 1–20% of a covalent C−C bond).[13]

Terpyridine−metal complexes are widely applied building blocks in supramolecular and macromolecular chemistry. Generally, 2,2′:6′,2″-terpyridines (tpy) are tridentate ligands which can complex a variety of transition metal ions with a high binding constant (compared to phenanthroline or 2,2′-bipyridine ligands), leading to the formation of octahedral metal complexes without giving rise to enantiomers.[14,15] The various possibilities for the functionalization of terpyridine ligands in the 4′-position[16,17] allows a straightforward access to supramolecular monomers and polymers.[18,19] The success in controlling the formation of a certain supramolecular metal-containing structure lies in the careful choice of metal ion, ligand, and framework motifs.[20–24]

Recently, we showed that the polymerization of a bis-terpyridine monomer with $RuCl_3$ and a mono-terpyridine functionalized polymer can lead to supramolecular triblock copolymers in a one-step procedure,[25] thereby expanding the range of accessible supramolecular polymer architectures.

Here, we describe in detail the synthesis of A-*b*-B-*b*-A triblock copolymers based on a $tpy_2M(II)$ connectivity with three transition metal ions characterized by different binding strengths.[26,40] The use of different metal ions offers the possibility of designing new materials with different stabilities, an aspect which could be used for the preparation of switchable systems. Finally, the micellization of the accordingly synthesized amphiphilic A-*b*-B-*b*-A triblock copolymers in a mixture of acetone and water was studied by dynamic light scattering (DLS) and cryo-transmission electron microscopy (cryo-TEM).

Experimental Part

Materials and General Experimental Details. All reactions were performed under an inert atmosphere of argon using conical glass vials that can be capped with a septum. All chemicals were of reagent grade and used as received unless otherwise specified. α-Methoxy-ω-hydroxypoly(ethylene glycol), ammonium hexafluorophosphate, Ni(II), Co(II), and Fe(II) acetate, and Ni(II), Co(II), and Fe(II) chloride were purchased from Aldrich. 1,16-Hexadecanediol was purchased from Fluka. 4′-Chloroterpyridine was synthesized as described previously.[27] Preparative size-exclusion chromatography was performed on BioBeads S-X1 columns using dichloromethane or acetone as eluent.

Instrumentation. Size exclusion chromatograms were measured on a Waters SEC system consisting of an isocratic pump, solvent degasser, column oven, 2996 photodiode array (PDA) detector, 2414 refractive index detector, 717 plus autosampler, and a Styragel HT 4 GPC column with a precolumn installed. The eluent was *N*,*N*-dimethylformamide (DMF) with 5 mM NH_4PF_6 at a flow speed of 0.5 mL/min; a linear PEG calibration was used. The column temperature was 50 °C.

* Corresponding author: Fax (+31) (0)40 2474186; e-mail u.s.schubert@tue.nl.
[†] Eindhoven University of Technology and Dutch Polymer Institute.
[‡] Université catholique de Louvain.
[§] Friedrich-Schiller-Universität Jena.

10.1021/ma0718954 CCC: $40.75
Published on Web 03/19/2008

Scheme 1. Schematic Representation of the Synthesis of Mono-terpyridine-PEG 4, 1,16-Bis(2,2′:6′,2″-terpyridin-4′-yloxy)hexadecane 5, Ni(II) Chain Extended Polymer 7, and Bis(α-terpyridine-ω-methylpoly(ethylene glycol)Ni(II) Hexafluorophospate 6

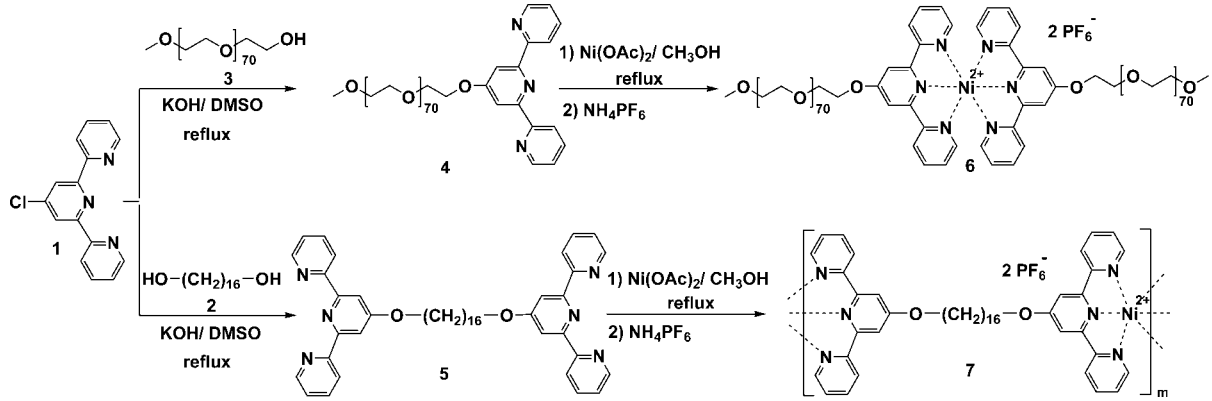

Scheme 2. Schematic Representation of the Synthesis of the Ni(II), Fe(II), and Co(II) A-*b*-B-*b*-A Triblock Copolymers 8a−d, 9, and 10 via Methods A and B

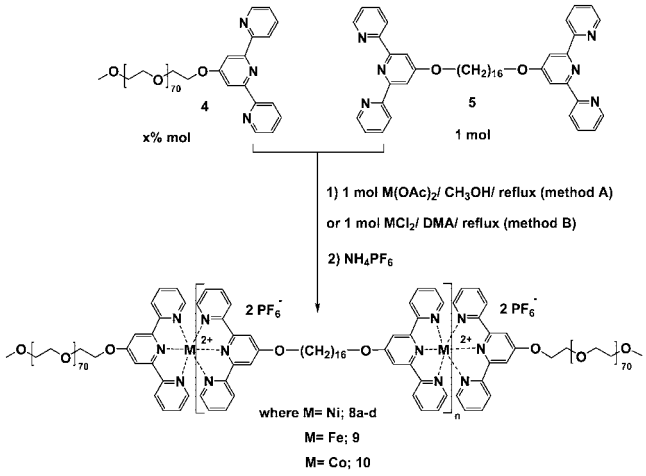

Nuclear magnetic resonance spectra were recorded on a Varian Gemini 400 MHz spectrometer at 298 K. Chemical shifts are reported in parts per million (δ) downfield from an internal standard, tetramethylsilane (TMS) in CD_3COCD_3.

Dynamic light scattering (DLS) experiments were performed on a Malvern CGS-3 equipped with a He−Ne laser (633 nm). The measurements have been performed at an angle of 90° and at a temperature of 25 °C. The viscosity of the 1:1 mixture of acetone and water was measured with a Cannon-Fenske viscometer (size 50). The density of the mixture was measured using a pycnometer (Brand) having a bulb volume of 10 cm^3. The results were analyzed by the CONTIN method, which is based on an inverse-Laplace transformation of the data and which gives access to a size distribution histogram for the analyzed micellar solutions. Cryogenic transmission electron microscopy (cryo-TEM) measurements were performed on a FEI Tecnai 20, type Sphera TEM operating at 200 kV (LaB6 filament). Images were recorded with a bottom mounted 1K × 1K Gatan CCD camera. A Gatan cryoholder operating at −170 °C was used for the cryo-TEM measurements. R2/2 Quantifoil Jena grids were purchased from SPI. Cryo-TEM specimens were prepared applying 3 μL aliquots to the grids within the environmental chamber (22 °C, relative humidity 100%) of an automated vitrification robot (FEI Vitrobot Mark III). Excess liquid was blotted away (−2 mm offset, 2.5 s) with filter paper within the environmental chamber of the Vitrobot. The grids were subsequently shot through a shutter into melting ethane placed just outside the environmental chamber. Vitrified specimens were stored under liquid nitrogen before imaging. Prior to blotting, the grids were made hydrophilic by surface plasma treatment using a Cressington 208 carbon coater operating at 5 mA for 40 s. For conventional sample preparation 3 μL aliquots were applied to a 200 mesh carbon-coated copper grid, and subsequently excess liquid was quickly manually blotted away with filter paper.

Synthesis of Mono-terpyridine End-Functionalized Poly(ethylene glycol), 4. Compound **4** has been prepared according to literature procedures.[31] Yield: 93%. ^{1}H NMR (400 MHz, CD_3COCD_3, 25 °C): δ = 8.71 (m, 4H, H^6, $H^{6''}$, H^3, $H^{3''}$), 8.12 (s, 2H, $H^{3'}$, $H^{5'}$), 7.98 (td, 2H, J = 7.8, 1.6 Hz; H^4, $H^{4''}$), 7.46 (td, 2H, J = 8.0, 2.0 Hz; H^5, $H^{5''}$), 4.44 (m, 2H, tpyOC H_2), 3.96 (m, 2H, tpyOCH$_2$CH_2), 3.62–3.48 (m, 60 H, PEG backbone), 3.31 (s, 3H, OCH_3). SEC: $\bar{M}_n$ = 3300 g mol^{-1}; $\bar{M}_w$ = 3650 g mol^{-1}, PDI = 1.11.

Synthesis of 1,16-Bis(2,2′:6′,2″-terpyridin-4′-yloxy)hexadecane, 5. Compound **5** was synthesized according to literature procedures.[25,28] Yield: 88%. ^{1}H NMR (400 MHz, CD_3COCD_3, 25 °C): δ = 8.67 (m, 8H, H^6, $H^{6''}$, H^3, $H^{3''}$), 8.08 (s, 4H, $H^{3'}$, $H^{5'}$), 7.95 (td, 4H, J = 7.6, 2.0 Hz; H^4, $H^{4''}$), 7.44 (td, 4H, J = 5.9, 1.8 Hz; H^5, $H^{5''}$), 4.28 (t, 4H, J = 6.2 Hz, tpy OC H_2), 1.89 (m, 4 H, OCH$_2$CH_2), 1.55 (m, 4 H, OCH$_2$CH$_2$CH_2), 1.3–1.42 (m, 20 H, OCH$_2$CH$_2$CH$_2$(CH_2)$_{10}$−CH$_2$CH$_2$CH$_2$O). MALDI-TOF-MS (matrix: dithranol), m/z (%)) 21.9 (MH^+, 35%), 743.9 (MNa^+, 100%).

Synthesis of Bis(α-terpyridine-ω-methylpoly(ethylene glycol)nickel(II) Hexafluorophospate, 6. Compound **6** was prepared as described previously.[30,31] Yield: 25%. Because of the paramagnetic metal complex, the ^{1}H NMR spectrum showed only the polymer backbone. In the aromatic region no signals from uncomplexed terpyridine were observed, indicating full complexation of the starting material **4**. SEC: $\bar{M}_n$ = 8100 g mol^{-1}; $\bar{M}_w$ = 8700 g mol^{-1}, PDI = 1.07.

General Synthesis of A-*b*-B-*b*-A Triblock Copolymers 8, 9, and 10 (Method A). M(OAc)$_2$·H$_2$O (0.063 mmol), mono-terpyridine end-functionalized poly(ethylene glycol) **4** (variation of the end-capper from 0% to 80% molar percentages in comparison to the M(OAc)$_2$ and monomer **5**), and 1,16-bis(2,2′:6′,2″-terpyridin-4′-yloxy)hexadecane **5** (43.26 mg, 0.06 mmol) were added to 300 μL of MeOH in a conical glass vial and capped with a septum. The polymerization was performed overnight at 65 °C. A 10-fold excess of NH_4PF_6 (15.686 mg, 0.63 mmol) in 2 mL of MeOH was added to the solution, and the stirring was continued for 1 h, after which the solvent was evaporated. It was observed that this counterion exchange had a significant effect on the solubility of the synthesized polymers; with acetate counterions they were methanol-soluble and acetone-insoluble, while with hexafluorophosphate counterions the reverse behavior was observed. The excess of NH_4PF_6 was removed by preparative size exclusion chromatography in acetone. The pure compounds were obtained by precipitation from acetone into dichloromethane.

Synthesis of A-*b*-B-*b*-A Triblock Copolymers 8, 9, and 10 (Method B). MCl$_2$·H$_2$O (0.315 mmol), 1,16-bis(2,2′:6′,2″-terpyridin-4′-yloxy)hexadecane **5** (0.3 mmol, 216.3 mg), and α-terpy-

Table 1. Estimation of the Molecular Weight Values and Polydispersity Indexes for 3, 4, and Crude A-*b*-B-*b*-A 8a−d Triblock Copolymers (Where 8a is A-*b*-B-*b*-A with 10% End-Capper 4; 8b is A-*b*-B-*b*-A with 20% End-Capper 4; 8c is A-*b*-B-*b*-A with 40% End-Capper 4; 8d is A-*b*-B-*b*-A with 80% End-Capper 4) Using Size Exclusion Chromatography with PEG Calibration

compound	M_n (g/mol)	M_w (g/mol)	PDI
4	3300	3650	1.11
6	8100	8700	1.07
7	8100	14500	1.80
8a	12350	24000	1.94
8b	10400	18050	1.73
8c	7300	12900	1.76
8d	6400	10700	1.67

ridine-ω-methyl-poly(ethylene glycol) **4** ($\bar{M}_n = 3000$ g mol^{-1}, 0.03 mmol, 90 mg) were added to 1.5 mL of dimethylacetamide (DMA) in conical glass vials and capped with a septum. All components became readily dissolved after stirring the mixture for 3 min at 70 °C. The polymerization was performed overnight at 130 °C. The resulting product was purified as in the first approach after adding a 10-fold excess of NH_4PF_6 (see method A).

Micelle Preparation of A-*b*-B-*b*-A Triblock Copolymers 8, 9, and 10. Since the block copolymers were not readily soluble in water, they were first dissolved in acetone (1 g/L). A water volume equal to half of the acetone volume was then added under stirring by steps of 50 μL, followed by the addition of the same water volume in one shot. The solutions were analyzed immediately without filtration.

Results and Discussion

In order to prepare supramolecular, terpyridine containing, A-*b*-B-*b*-A triblock copolymers, the polycondensation-like polymerization conditions of a α,ω-bis-terpyridine monomer with $RuCl_3$ were recently optimized in a parallel fashion with the appropriate screening techniques (an optimized SEC system and an UV–vis plate reader).[29] Here, we apply the same approach for the formation of A-*b*-B-*b*-A supramolecular triblock copolymers based on tpy_2Ni(II), tpy_2Fe(II), and tpy_2Co(II) connectivities and study the micellization of these new materials. The chemical structure of the synthesized metallo-supramolecular A-*b*-B-*b*-A triblock copolymers **8a−d**, **9**, and **10**, consisting of terpyridine modified poly(ethylene glycol) A blocks and a poly(1,16-bis(2,2′:6′,2″-terpyridin-4′-yloxy)hexadecane) B central block, is depicted in Scheme 2.

To get an insight in the factors influencing the polycondensation reaction, optimization reactions were performed on the most stable system of the present study, namely tpy_2Ni(II). Indeed, we recently showed that nickel binds stronger than iron, whereas cobalt offers the weakest supramolecular connectivity in this series.[30] First of all, Ni(II) homopolymer **6** was prepared by complexing ligand **4** with $Ni(OAc)_2$ in refluxing MeOH (Scheme 1).[30,31] The main characterization technique for the Ni(II) homopolymer **6** (and all other nickel-containing polymers) was SEC (Table 1) since ^{1}H NMR could not detect any peaks in the aromatic region of these species due to the paramagnetic characteristic of Ni^{2+}. Homopolymer **6** was used in the following research as a reference compound. Subsequently, the A-*b*-B-*b*-A triblock copolymer **8** based on tpy_2Ni(II) was prepared. Several synthetic procedures have been investigated. The DMA procedure (method B) with nickel(II) chloride, as described for the tpy_2Ru(II) connectivity,[25] was less successful in the tpy_2Ni(II) case and was leading to low molecular weight block copolymers (as observed by SEC). Changing nickel(II) chloride to nickel(II) acetate but keeping the same solvent did not improve the polymerization results. In fact, it was observed from SEC measurements that no product was formed. One explanation could be related with the capacity of the solvent (DMA) to compete for the coordination,[32] since nickel ions are not binding to the terpyridine as strongly as ruthenium ions.[25] Moreover, the low solubility of Ni(II) chloride and later also acetate in the reaction mixture as well as the influence of the used counterions in the present polycondensation reactions should not be neglected.[37] Taking into account previously gained knowledge regarding the chain extended polymerization based on tpy_2Ni(II),[30] the reaction solvent (DMA) was changed to methanol yielding in the formation of a polymer, confirming once again the crucial role of the solvent in the polymerization process.

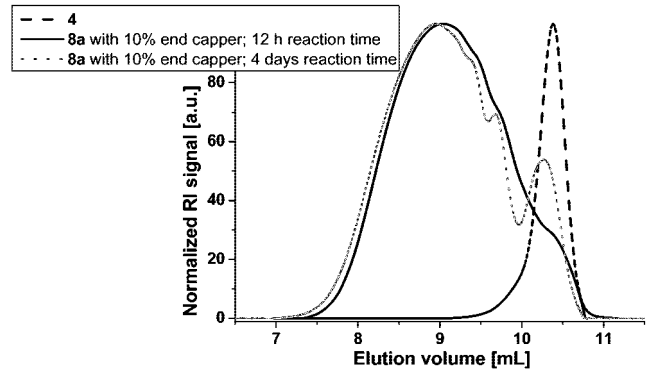

Figure 1. SEC elution curves (RI detector) showing the influence of the reaction time on the molecular weight of the A-*b*-B-*b*-A **8a** triblock copolymers with 10% of the end-capper **4**.

Since the "metallo-polymerization" of **5** would lead to the formation of chain-extended polymers (compare **7**), the addition of a macromolecular chain stopper, such as **4**, should allow the formation of A-*b*-B-*b*-A architectures. Chain terminators are frequently used in technical polycondensation processes in order to control the molecular weights. Moreover, the addition of various amounts of **4** should result in A-*b*-B-*b*-A copolymers with different lengths of the B block as it is known from classical polycondensation reactions.[34] As we were mainly interested in linear high molecular weight A-*b*-B-*b*-A block copolymers, the addition of the chain terminator **4** could help us to reduce/limit the possibility of forming macrocycles.[34]

First of all, for the A-*b*-B-*b*-A triblock copolymer **8a** with 10% end-capper **4**, the influence of the reaction time on the molecular weight was studied. The polycondensation reaction was monitored during the first 12 h. From SEC analysis it was observed that the metallo-polycondensation of the studied system first leads to low molecular weight species that couple in time leading to higher molecular weight block copolymers, in agreement with the results presented in the literature for typical chain step polymerization.[33,34] Moreover, SEC analysis also revealed (see Figure 1) that after 12 h the molecular weight did not increase anymore and that much longer reaction times (e.g., 4 days) led to lower molecular weight species that are most likely of macrocyclic nature,[28] in addition to the linear A-*b*-B-*b*-A triblock copolymers. This observation is in agreement with the results presented in the literature for the preparation of polyesters via step growth polymerization.[35,36] This aspect might be due to the fact that this polycondensation is an equilibrium reaction, and the proportion of rings may also vary with time being thermodynamically more favored.[34,37] By this assumption we can presume that during the polycondensation reaction the linear triblock copolymer might be first formed and then, in time due to the (possible) dynamic equilibrium between linear and cyclic macromolecules, rings are formed as well.[34] As we were interested mainly in the preparation of linear triblock copolymers, we decided to select the optimal reaction time of 12 h, in terms of molecular weight buildup, for the rest of the polycondensation reactions.

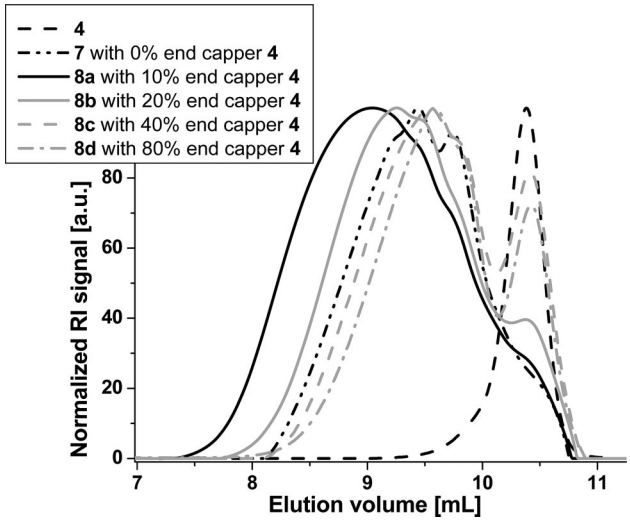

Figure 2. SEC elution curves (RI detector) for the mono-terpyridine-PEG **4** and the corresponding A-*b*-B-*b*-A **8a**−**d** triblock copolymers with different percentages of the end-capper **4** after 12 h reaction time.

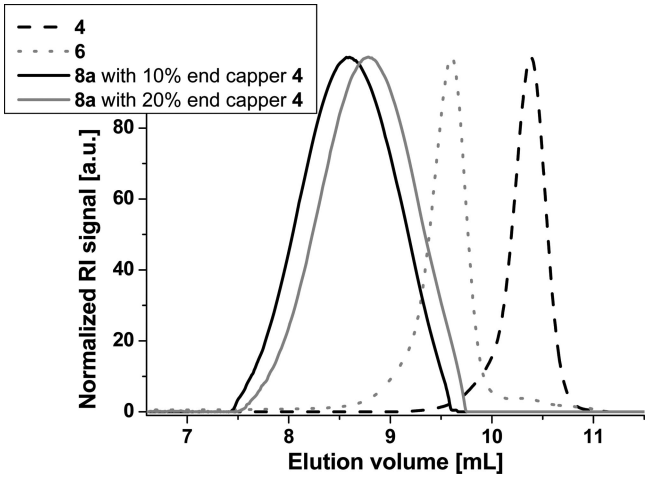

Figure 3. SEC elution curves (RI detector) for the mono-terpyridine-PEG **4**, Ni(II) homopolymer **6**, and the purified A-*b*-B-*b*-A **8a,b** triblock copolymers with 10% and 20% end-capper **4**.

The synthesis of **8a**−**d** with different molar ratios of the end-capper **4** was thus performed in methanol for 12 h. The accordingly synthesized copolymers were characterized by SEC. Considering the composition of the triblock copolymers, no proper GPC calibration standard could be found for these systems. However, to give an indication of molar mass and polydispersity index, Table 1 shows the molecular weights of the A-*b*-B-*b*-A triblock copolymers **8a**−**d** with different percentages of the end-capper **4** calculated with a PEG calibration. As it can be seen from Table 1 and from the SEC traces in Figure 2, the highest molecular weights were obtained by the addition of 10% of the end-capper **4**. As expected, further increase of the amount of **4** in the polycondensation reaction led to the formation of shorter block copolymers with respectively lower molecular weights.

Subsequent purification (BioBeads S-X1 in acetone and precipitation from acetone into dichloromethane) of the crude materials removed the macrocycles possibly formed during the polymerization reactions (Figure 3). The absence of aromatic protons in the ^{1}H NMR spectrum showed that no uncomplexed monomers are present in the final A-*b*-B-*b*-A triblock copolymers. Furthermore, results obtained from the SEC-coupled in-line diode array detector demonstrate the integrity of the supramolecular assembly over the complete distribution as indicated by the ligand-centered (LC) $\pi-\pi^*$ absorption bands around 317 and 310 nm (Figure 4). The purified A-*b*-B-*b*-A triblock copolymer **8a** with the highest molecular weight obtained in this study was further used for micellization studies.

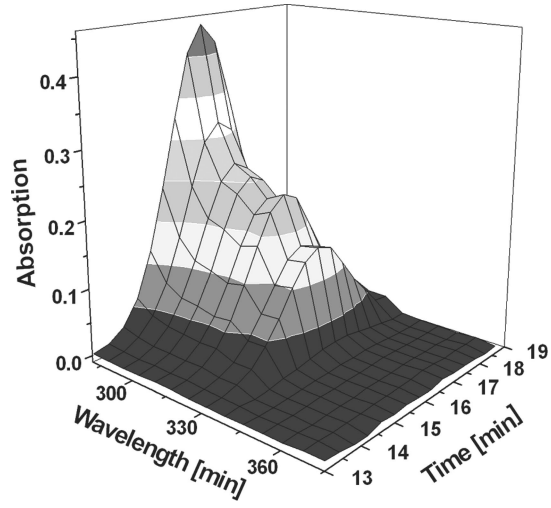

Figure 4. SEC elution curve (PDA detector) for the purified A-*b*-B-*b*-A **8a** triblock copolymer with 10% end-capper **4**.

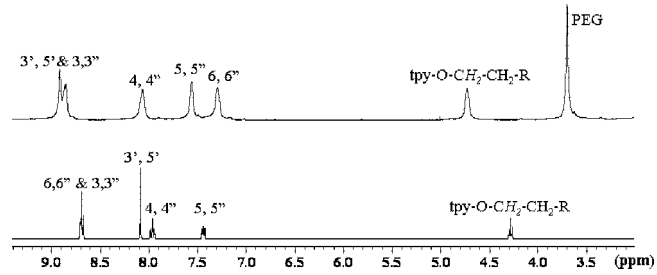

Figure 5. Comparison between the ^{1}H NMR spectra of monomer **5** (bottom) and A-*b*-B-*b*-A triblock copolymer **9** obtained via method B (top) in acetone-d_6.

With this knowledge regarding the synthesis, stability, and characterization of A-*b*-B-*b*-A triblock copolymers **8a**−**d** based on tpy$_2$Ni(II), we focused our attention on the preparation of A-*b*-B-*b*-A triblock copolymers based on tpy$_2$Fe(II) connectivity. For this system the two different synthetic approaches (methods A and B) have been studied, and the results were compared. The first one followed the preparation of the triblock copolymer based on tpy$_2$Ru(II) using 10% of the end-capper[25] (see Experimental Part: method B), and the second one followed the successful synthesis of the triblock copolymer described earlier for tpy$_2$Ni(II), also with 10% end-capper (see Experimental Part: method A). As a result of the weaker binding strength of the bis(terpyridine)iron(II) complex, as compared to the analogous ruthenium and nickel complexes, it is unfortunately not possible to perform SEC investigations on such polymers.[30] For this reason the main characterization technique for the tpy$_2$Fe(II) block copolymers was ^{1}H NMR. For the purified A-*b*-B-*b*-A triblock copolymer based on tpy$_2$Fe(II) **9** (prepared by the DMA approach) the ^{1}H NMR (Figure 5) revealed similar degrees of polymerization as in the case of the ruthenium polymers described elsewhere.[25] Assuming that both ends of 1,16-bis(2,2′:6′,2″-terpyridin-4′-yloxy)hexadecane **5** were functionalized with PEG in order to obtain the A-*b*-B-*b*-A triblock copolymer structure, the ratio of signal intensities belonging to the PEG as well as 1,16-bis(2,2′:6′,2″-terpyridin-4′-yloxy)hexadecane revealed a degree of polymerization of

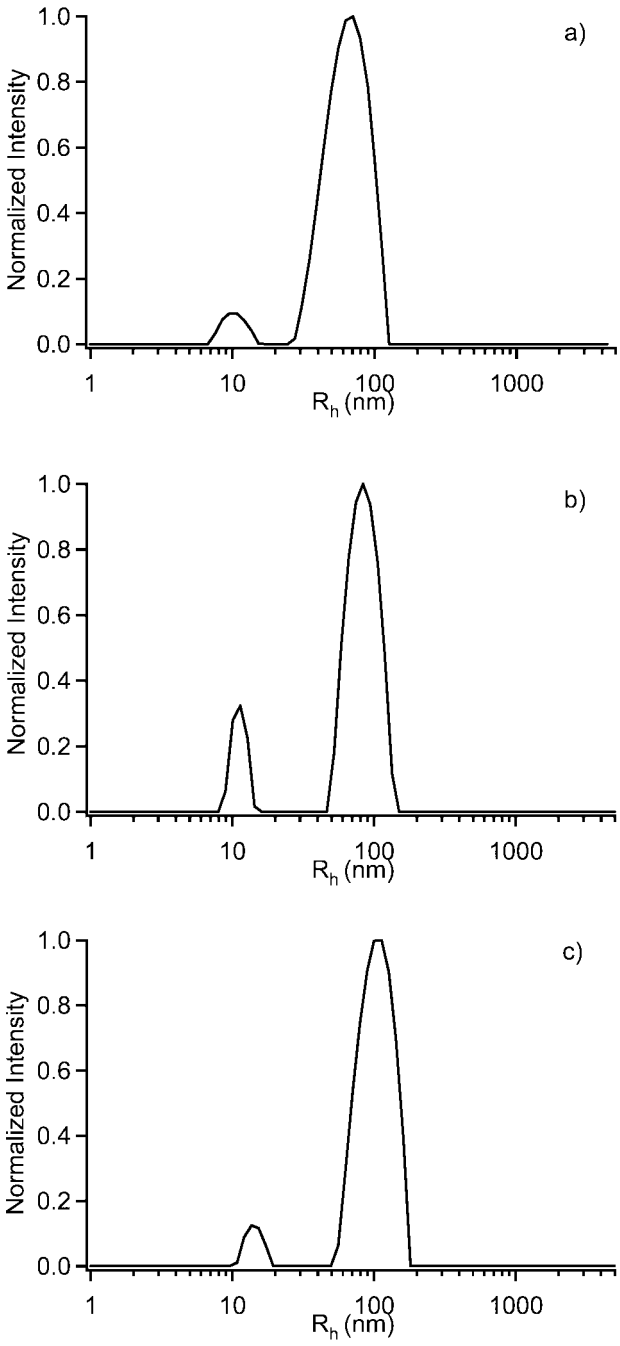

Figure 6. CONTIN size distribution histograms obtained on the micelles prepared from the A-*b*-B-*b*-A triblock copolymers **8a**, **9**, and **10** in an acetone/water mixture: (a) copolymer **8a** based on $tpy_2Ni(II)$, (b) copolymer **9** based on $tpy_2Fe(II)$, (c) copolymer **10** based on $tpy_2Co(II)$.

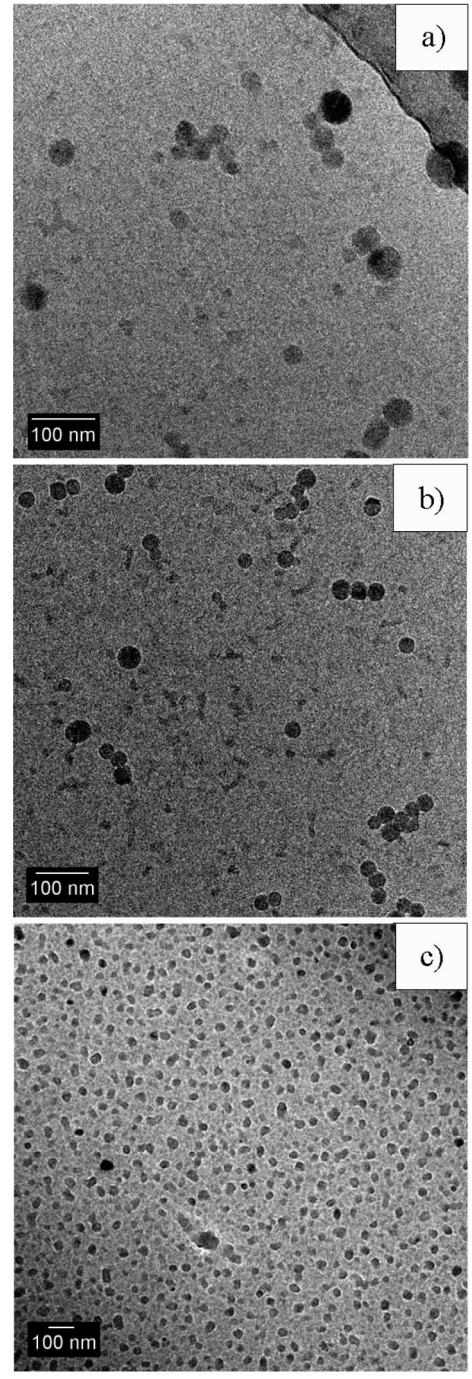

Figure 7. Cryo-TEM picture of micelles prepared from the A-*b*-B-*b*-A triblock copolymers **8a**, **9**, and **10** in an acetone/water mixture: (a) copolymer **8a** based on $tpy_2Ni(II)$, (b) copolymer **9** based on $tpy_2Fe(II)$, (c) copolymer **10** based on $tpy_2Co(II)$.

the central B block of ~40 units (compared to 33 units for the corresponding ruthenium-containing polymer).[25] Therefore, the number-average molecular weight of polymer **9** can be calculated to be 35 kDa if the PF_6^- counterions are omitted and 46.5 kDa if they are taken into account. Furthermore, almost full complexation was observed in the polymer as revealed by a downfield shift of the methylene protons next to the terpyridine units (from 4.29 ppm (uncomplexed) to 4.72 ppm (complexed)) in the ^1H NMR spectrum. Figure 5 reveals that less than 3% uncomplexed terpyridine moieties are present in polymer **9**, which might belong to AB-type block copolymer or polyB structures. Moreover, the UV–vis spectrum shows the typical metal-to-ligand-charge-transfer band of the iron(II)−bis(terpyridine) type of connectivity in the visible region (560 nm), indicating that the anticipated connectivities are actually formed. This sample was further used in micellization studies.

The second approach followed for the preparation of block copolymer **9** with 10% end-capper **4** was the one used for the synthesis of **8a**: in methanol with iron(II) acetate (see Experimental Part: method A). From the ^1H NMR spectrum the degree of polymerization was found to be smaller (~13 units for the B block) than with the DMA approach. One explanation could be the lower temperature in the methanol approach compared to the DMA approach, yielding lower molecular weights. Unfortunately, the methanol approach does not allow reaction temperatures higher than ~65 °C, and at temperatures lower

than 70 °C the reaction in DMA was not homogeneous, preventing a detailed study of this effect.

The last system for our study was the A-*b*-B-*b*-A block copolymers based on the $tpy_2Co(II)$ connectivity using 10% end-capper **4** as A block. The two synthetic approaches have been also investigated and compared (see Experimental Part: methods A and B). As a result of previous studies performed on the bis(terpyridine)cobalt(II) homopolymer complexes,[30] it is known that it is not possible to perform size exclusion chromatographic investigations with these copolymers due to the rather low stability of the bis(terpyridine)Co(II) complex.[30] Therefore, the $tpy_2Co(II)$ block copolymers were characterized mainly by ^1H NMR. It is known that paramagnetic complexes, such as Ni(II) and Co(II), have unpaired electrons giving rise to two main effects in the ^1H NMR spectrum. On the one hand, the local magnetic field at the protons is significantly different from the applied field due to the presence of unpaired electrons at the metal center. On the other hand, the recorded signals in the proton ^1H NMR are broadened as a result of interaction between the nuclear spins and the electron spins providing an efficient relaxation mechanism.[38] For $tpy_2Ni(II)$ the relaxation is very fast, and the signals are so broadened that they cannot be observed anymore. For $tpy_2Co(II)$ the signals in the ^1H NMR spectrum should normally reveal a Knight shift (up to 200 ppm from TMS).[39–41] In the case of the prepared Co(II) block copolymers **10** (methods A and B), no signals could, however, be observed in the mentioned region. The absence of the expected signals could be explained by the high molecular weight of **10**, which would decrease the chain mobility and the diffusion rates during the ^1H NMR measurements, inducing a broadening of the terpyridine signals, which normally appears at 100 ppm in a bis(terpyridine)cobalt(II) model complex (Knight shift),[30,39] and preventing their detection. From the comparison of the ^1H NMR spectra for the two A-*b*-B-*b*-A block copolymers **10** prepared via methods A and B, we concluded that the acetate approach (method A) led to a higher molecular weight block copolymer (almost full conversion for the B block) in comparison with the DMA approach (less than 30% of the B block was incorporated into the synthesized triblock copolymer). The UV–vis spectrum of **10** (obtained via method A) showed also the ligand-centered (LC) $\pi-\pi^*$ absorption bands in the visible region around 322 and 340 nm which are characteristic for $tpy_2Co(II)$ connectivity. This sample was further used for micellization studies.

In order to study the amphiphilic character of the supramolecular triblock copolymers **8a**, **9**, and **10**, their ability to form micelles was investigated. Since the supramolecular block copolymers were not readily soluble in water, the micelles were prepared by first dissolving the block copolymers **8a**, **9**, and **10** (with the highest available molecular weights) in acetone, which is a good solvent for both blocks, followed by the gradual addition of water, which is a selective solvent for the PEG-containing block and a precipitant for the other block. Upon addition of water, the insoluble block collapses and aggregates are formed, shielded from the solvent by a corona of the PEG blocks. To transfer the micelles into pure water, we tried to remove the acetone by slow evaporation and by dialysis against water, but both methods lead to the precipitation of the copolymers. The micelles formed in the acetone/water (50/50) mixture were then characterized by dynamic light scattering (DLS) and cryo-TEM.

The CONTIN analysis of the DLS results obtained on the micelles from the three copolymers revealed the presence of two different populations (Figure 6). The first population has a hydrodynamic radius of ~10 nm for all three copolymers, and the second population has a R_h around 100 nm for copolymer based on Co(II), around 84 nm for the copolymer based on Fe(II), and around 56 nm for the copolymer based on Ni(II). The first population could correspond to isolated, non-aggregated, copolymer chains while the second one is attributed to micelles.

The micelles formed by the supramolecular triblocks were imaged by cryo-TEM. Figure 7 shows the micelles of the supramolecular triblock based on $tpy_2Ni(II)$, $tpy_2Fe(II)$, and $tpy_2Co(II)$ connectivity, imaged by cryo-TEM. Spherical objects with a radius in the range of 10−14 nm are observed for all copolymers together with a few larger aggregates. These data confirm that the population of large size observed in the DLS experiments is attributed to micelles. Cryo-TEM indeed measures the core of the micelles and should thus give smaller sizes compared to DLS. However, the core radii measured by cryo-TEM seem quite small compared to the size of the entire micelles measured by DLS, and moreover there is no clear variation of size according to the metal as it is observed by DLS. In conclusion, the amphiphilic nature of the copolymers is clearly demonstrated by their ability to form micelles in water; however, a more in-depth investigation is required to clarify the exact structure of those objects.

Conclusion

The presented results clearly demonstrate that A-*b*-B-*b*-A triblock copolymers based on $tpy_2M(II)$ connectivity can be prepared with different metal ions via a simple one-step polycondensation approach. The optimization studies performed with different amounts of end-capper, for the case of $tpy_2Ni(II)$ connectivity, led to a variation in length of the $tpy_2Ni(II)$ A-*b*-B-*b*-A triblock copolymers. All the prepared metallo-triblock copolymers **8a**, **9**, and **10** containing 10% end-capper **4** are amphiphilic, and they can form micelles in acetone/water mixtures following a simple preparation approach. The resulting micelles were analyzed by cryo-TEM and DLS. The imaging results showed the formation of micelles as a proof of the amphiphilicity of the prepared block copolymers. In the future, it will be very interesting to apply this knowledge for the synthesis and application of designed stimuli-responsive micelles, since the strength of the metal–ligand interaction can be easily tuned due to the selection of the metal ion (and/or the exchange of counterions).

Acknowledgment. This study was supported by the Dutch Polymer Institute (DPI project #447) and the Nederlandse Organisatie voor Wetenschappelijk Onderzoek (NWO, open competition and VICI award for U.S. S.). CAF is Research Associate of the FRS-FNRS. J.F.G. thanks the ESF STIPOMAT Programme.

References and Notes

(1) Lehn, J.-M. *Polym. Int.* **2002**, *51*, 825–839.
(2) Brunsveld, L.; Folmer, B. J. B.; Meijer, E. W.; Sijbesma, R. P. *Chem. Rev.* **2001**, *101*, 4071–4097.
(3) Yang, X.; Hua, F.; Yamato, K.; Ruckenstein, E.; Gong, B.; Kim, W.; Ryu, C. Y. *Angew. Chem., Int. Ed.* **2004**, *43*, 6471–6474.
(4) Sijbesma, R. P.; Beijer, F. H.; Brunsveld, L.; Folmer, B. J. B.; Ky Hirschberg, J. H. K.; Lange, R. F. M.; Lowe, J. K. L.; Meijer, E. W. *Science* **1997**, *278*, 1601–1604.
(5) Schmuck, C.; Wienand, W. *Angew. Chem., Int. Ed.* **2001**, *40*, 4363–4369.
(6) Yamauchi, K.; Lizotte, J. R.; Long, T. E. *Macromolecules* **2002**, *35*, 8745–8750.
(7) (a) Schubert, U. S.; Eschbaumer, C. *Angew. Chem., Int. Ed.* **2002**, *41*, 2892–2926. (b) Fustin, C. A.; Guillet, P.; Schubert, U. S.; Gohy, J. F. *Adv. Mater.* **2007**, *19*, 1665–1673.
(8) Beck, J. B.; Ineman, J. M.; Rowan, S. J. *Macromolecules* **2005**, *38*, 5060–5068.
(9) Hofmeier, H.; Schmatloch, S.; Wouters, D.; Schubert, U. S. *Macromol. Chem. Phys.* **2003**, *204*, 2197–2203.

(10) Russell, T. P.; Jerome, R.; Charlier, P.; Foucart, M. *Macromolecules* **1988**, *21*, 1709–1717.
(11) Guan, Y.; Yu, S.-H.; Antonietti, M.; Böttcher, C.; Faul, C. F. J. *Chem.—Eur. J.* **2005**, *11*, 1305–1311.
(12) Sheng, Y.; Uwe, B.; Tobias, G.; Marina, L.; Würthner, F. *J. Am. Chem. Soc.* **2004**, *126*, 8336–8348.
(13) Goshe, A. J.; Steele, I. M.; Ceccarelli, C.; Rheingold, A. L.; Bosnich, B. *Proc. Natl. Acad. Sci. U.S.A.* **2002**, *99*, 4823–2829.
(14) Constable, E. C. *Macromol. Symp.* **1995**, *98*, 503–524.
(15) Constable, E. C.; Cargill Thompson, A. M. W. *J. Chem. Soc., Dalton Trans.* **1992**, *3467*, 3475.
(16) Schubert, U. S.; Eschbaumer, C.; Hien, O.; Andres, P. R. *Tetrahedron Lett.* **2001**, *42*, 4705–4707.
(17) Heller, M.; Schubert, U. S. *Eur. J. Org. Chem.* **2003**, *6*, 47–61.
(18) Schubert, U. S.; Eschbaumer, C. *Macromol. Symp.* **2001**, *163*, 177–187.
(19) Schubert, U. S.; Eschbaumer, C.; Andres, P.; Hofmeier, H.; Weidl, C. H.; Herdtweck, E.; Dulkeith, E.; Morteani, A.; Hecker, N.; Feldmann, J. *Synth. Met.* **2001**, *121*, 1249–1252.
(20) Ye, B.-H.; Tong, M.-L.; Chen, X.-M. *Coord. Chem. Rev.* **2005**, *249*, 545–565.
(21) Kelch, S.; Rehahn, M. *Macromolecules* **1999**, *32*, 5818–5828.
(22) Dobrawa, R.; Würthner, F *Chem. Commun.* **2002**, *17*, 1878–1879.
(23) Schmatloch, S.; van den Berg, A. M. J.; Alexeev, A. S.; Hofmeier, H.; Schubert, U. S. *Macromolecules* **2003**, *36*, 9943–9949.
(24) Lohmeijer, B. G. G.; Schubert, U. S. *J. Polym. Sci., Part A: Polym. Chem.* **2003**, *41*, 1413–1427.
(25) Meier, M. A. R.; Wouters, D.; Ott, C.; Guillet, P.; Fustin, C.-A.; Gohy, J.-F.; Schubert, U. S. *Macromolecules* **2006**, *39*, 1569–1576.
(26) Holyer, R. H.; Hubbard, C. D.; Kettle, S. F. A.; Wilkins, R. G. *Inorg. Chem.* **1966**, *5*, 622–625.
(27) Schubert, U. S.; Schmatloch, S.; Precup, A. A. *Des. Monomers Polym.* **2002**, *5*, 211–221.
(28) Andres, P. R.; Schubert, U. S. *Synthesis* **2004**, *8*, 1229–1238.
(29) Meier, M. A. R.; Lohmeijer, B. G. G.; Schubert, U. S. *Macromol. Rapid Commun.* **2003**, *24*, 852–857.
(30) Chiper, M.; Meier, M. A. R.; Kranenburg, J. M.; Schubert, U. S. *Macromol. Chem. Phys.* **2007**, *208*, 679–689.
(31) Lohmeijer, B. G. G.; Schubert, U. S. *Macromol. Chem. Phys.* **2003**, *204*, 1072–1078.
(32) Dobrawa, R.; Würthner, F. *J. Polym. Sci., Part A: Polym. Chem.* **2005**, *43*, 4981–4995.
(33) Kricheldorf, H. R.; Rabenstein, M.; Maskos, M.; Schmidt, M. *Macromolecules* **2001**, *34*, 713–722.
(34) Kricheldorf, H. R.; Schwarz, G. *Macromol. Rapid Commun.* **2003**, *24*, 359–381.
(35) Kricheldorf, H. *Macromol. Symp.* **2003**, *199*, 1–13.
(36) Yokosawa, T.; Suzuki, H *J. Am. Chem. Soc.* **1999**, *121*, 11573–11574.
(37) Elias, H.-G. *An Introduction to Polymer Science*; Wiley-VCH: New York, 1997.
(38) Hore, P. J. *Nuclear Magnetic Resonance* (Oxford Chemistry Primers 32); Oxford University Press: Oxford, 1996.
(39) Constable, E. C.; Housecroft, C. E.; Kulke, T.; Lazzarini, C.; Schofield, E. R.; Zimmerman, Y. *Dalton Trans.* **2001**, *2864*, 2871.
(40) Hogg, R.; Wilkins, R. G. *J. Chem. Soc.* **1962**, *341*, 350.
(41) Epperson, J. D.; Ming, L.-J.; Baker, G. R.; Newkome, G. R. *J. Am. Chem. Soc.* **2001**, *123*, 8583–8592.

MA0718954